JACS Au
AN OPEN ACCESS JOURNAL OF THE AMERICAN CHEMICAL SOCIETY

pubs.acs.org/jacsau
Article

Interface Feedback Effect in Molecular Tunnel Junctions

Yunxia Feng, Jinwei Chen, Ioan Bâldea,* C. Daniel Frisbie,* and Zuoti Xie*

Cite This: JACS Au 2025, 5, 1258−1267

ABSTRACT: Despite numerous prior studies on molecular tunnel junctions, many important questions remain about the nature of metal−molecule contacts. Using the conducting probe atomic force microscope (CP-AFM) platform, we report here an investigation of electrical contact effects in junctions based on oligophenylene and alkyl dithiols (OPD*n*, *n* = 1, 2, 3 and C*n*DT, *n* = 8, 9, 10) linked via thiol anchoring groups to dissimilar Ag, Au, and Pt metal electrodes. Our data reveal a peculiar effect: the two metal−molecule interfaces "talk" to each other, *i.e.*, the choice of metal for the tip (t) electrode substantially changes the metal−HOMO electronic coupling Γ associated with the substrate (s) electrode, and vice versa. The metal−HOMO couplings Γ_t and Γ_s are not independent quantities. Their interdependence does not correlate with metal work function, chemisorption-driven work function change, or metal electronegativity, *i.e.*, properties characterizing charge transfer at the molecule−metal interface. Overall, our results reveal an undiscovered complexity associated with electrical contacts in molecular tunnel junctions that must be considered in theoretical descriptions and ongoing efforts to design junctions with specific electronic functions.

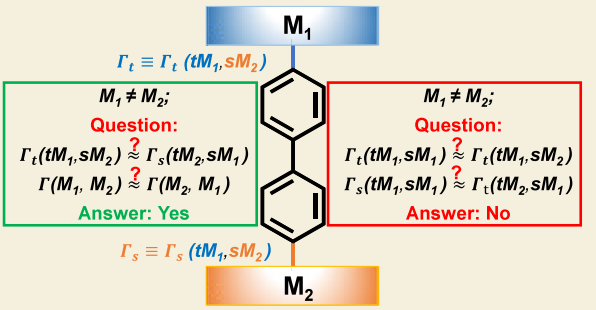

KEYWORDS: *molecular electronics, self-assembled monolayers, transport by tunneling, electronic coupling, interface feedback effect*

INTRODUCTION

Metal−molecule−metal tunnel junctions represent a major focus of molecular electronics and have attracted continuing interest over decades.[1−15] As the result of extensive efforts, it is possible to rationally design and fabricate molecular junctions with nanometer sizes that exhibit functions analogous to traditional inorganic semiconductor-based rectifiers,[16−19] transistors,[20−24] and switches.[25−30]

Despite these advances, there are many fundamental aspects of the current−voltage (*I*−*V*) behavior of molecular tunnel junctions (MTJs) that are not well understood. In particular, contact effects remain a critical area of investigation. Because of the nanoscopic nature of molecular tunnel junctions, electrical contacts can be anticipated to play a major role in junction *I*−*V* behavior. Indeed, in prior work the molecular electronics community has established that chemical contacts between molecules and electrodes through metal−S bonds, for example, lead to greater metal−molecular orbital (MO) coupling (Γ) and far higher conductance than "physical contacts", *e.g.*, metal−molecule van der Waals bonds.[31−33] It has also been shown that the choice of electrode material, *e.g.*, different metals such as Ag, Au, Pt, Hg, or eutectic GaIn alloy (EGaIn), can change junction conductance by orders of magnitude.[15,34−37] This is attributable to large changes in Γ. At the same time, it has been demonstrated that variation of electrode materials only weakly affects the energy offset (ε_h) of the frontier MO (*e.g.*, HOMO) from the junction Fermi level, a phenomenon known as "Fermi level pinning".[31−33,38,39] Thus, the effects of contacts on junction electronic structure and charge transport are profound, but as yet there is no theory that fully describes the observed behaviors.

Here we report an additional fascinating and critical observation about contacts in molecular tunnel junctions. Namely, we show that the MO electronic coupling Γ at one contact is deeply influenced by the MO electronic coupling to the second contact. That is, there is "cross-talk" or feedback between the two metal−molecule interfaces that plays a huge role in the overall junction conductance. As pointed out above, the general dependence of Γ on electrode choice has been demonstrated previously, but to our knowledge the interplay between the Γ values for the two distinct metal−molecule interfaces in an MTJ has not been reported before. We show that the interface feedback is not a function of interfacial metal−molecule charge transfer; there is no clear correlation of the effect with metal work function, or adsorption-induced change in metal work function, or metal electronegativity. Rather, we propose that this feedback is a direct consequence of the nontrivial charge redistribution within a molecule already adsorbed on an electrode upon contact with the second

Received: November 22, 2024
Revised: February 3, 2025
Accepted: February 3, 2025
Published: February 14, 2025

https://doi.org/10.1021/jacsau.4c01128
JACS Au 2025, 5, 1258−1267

electrode. Overall, our findings add to collective knowledge of contact effects in molecular junctions and also demonstrate an additional dimension of complexity that will have to be accounted for in any microscopic analysis of contact effects in MTJs.

RESULTS AND DISCUSSION

Model Systems

As a model system, we focus on MTJs based on self-assembled monolayers (SAMs) of centrosymmetric oligophenylene dithiol (OPD*n*) and alkyl dithiol (C*n*DT) molecules coupled to two metal contacts. The junctions are fabricated using the conducting probe atomic force microscopy (CP-AFM) platform, Figure 1. Figure S1 displays plots of the average *I*−*V*

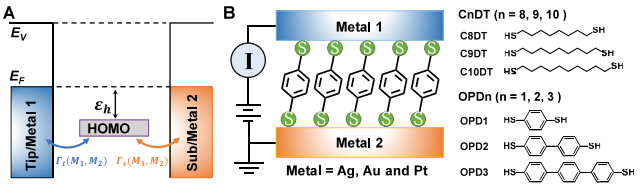

Figure 1. (A) Typical junction electronic structure with key parameters (HOMO level to Fermi level offset ε_h and molecule−electrode coupling strength Γ). (B) Schematic representation of the conducting probe atomic force microscopy (CP-AFM) setup. A metal coated AFM tip is brought into contact with a SAM of oligophenylene dithiol (OPD*n*, *n* = 1, 2, 3) or alkyl dithiol (C*n*DT, *n* = 8, 9, 10) on a metal coated substrate.

curves for the OPD*n* and C*n*DT junctions with different metal electrodes, *i.e.*, where the tip metal (t = Ag, Au, or Pt) is not the same as the substrate metal (s = Ag, Au, or Pt). Although the electrodes at the junction ends are different, the average *I*−*V* characteristics are practically symmetric upon reversing the bias polarity. Dissimilar electrodes do not make the current magnitude at positive bias (+*V* on the tip) visibly different from the current at negative bias (−*V* on the tip). This experimental observation is perhaps counterintuitive, but it is consistent with previous theoretical studies predicting that no significant current rectification in MTJs arises due to asymmetric molecule coupling to electrodes.[40,41] A deeper discussion of the implications of these results for models of rectification in MTJs will be the subject of another paper.

Theoretical Considerations

Previously, we have shown that the *I*−*V* characteristics of OPD*n* and C*n*DT junctions with similar metal contacts can be well described by the off-resonant single level model (orSLM),[33,42−48] which under specific assumptions (see below and Supporting Information for details) predicts that[48]

$$I = GV\frac{\varepsilon_0^2}{[\varepsilon_0(V)]^2 - (eV/2)^2} = GV\frac{\varepsilon_h^2}{(-\varepsilon_h + \gamma eV)^2 - \left(\frac{eV}{2}\right)^2} \quad (1)$$

where $\varepsilon_0 = -|\varepsilon_0| = -\varepsilon_h = E_{HOMO} - E_F < 0$) is the energy offset of the HOMO level that dominates the charge transport and *G* is the low bias conductance given by

$$G = NG_0\frac{\Gamma^2}{\varepsilon_h^2} \quad (2)$$

and

$$\Gamma \equiv \sqrt{\Gamma_s\Gamma_t} = \varepsilon_h\sqrt{G/(NG_0)} \quad (3)$$

Here Γ is an effective (more precisely, the geometric average of the) metal-MO electronic coupling and Γ_s, Γ_t are the couplings to the substrate and tip electrodes, ε_h is the HOMO-to-Fermi level offset, $G_0 = 2e^2/h = 77.48\ \mu S$ is the conductance quantum, γ is the orbital bias shift factor, and *N* is the number of molecules in the junction (the number of parallel conduction channels).

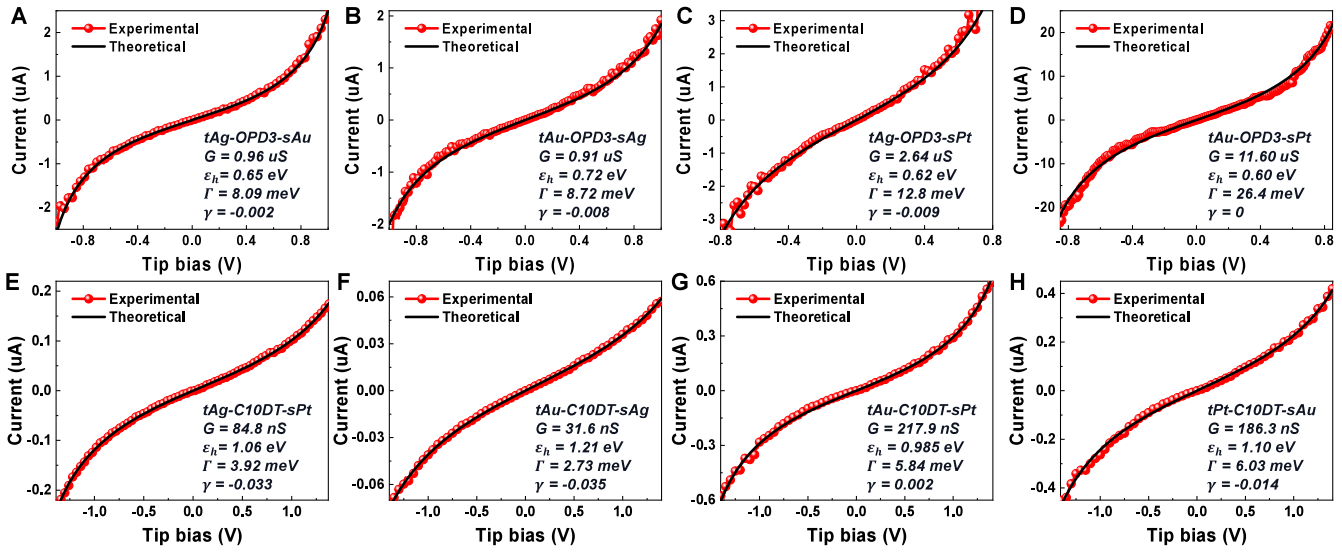

Figure 2. Good agreement between the individual CP-AFM *I*−*V* curves (red) for OPD3 and those obtained theoretically via eq 1 (black) is illustrated here for (A) Ag/Au, (B) Au/Ag, (C) Ag/Pt, and (D) Au/Pt (tip/substrate) junctions. For each junction, the three parameters needed in eq 1, low bias conductance *G* (1/R), energy offset ε_h, and orbital bias shift factor γ, are indicated in the legends. The values of the effective metal−MO coupling Γ were calculated from *G*, ε_h, *N*, and eq 1. (E−H) Similar results for C10DT and electrodes indicated in the inset.

https://doi.org/10.1021/jacsau.4c01128
JACS Au 2025, 5, 1258−1267

Table 1. Key Electronic Properties Extracted from Experiments on OPD*n* and C*n*DT-Based CP-AFM Junctions with Different Metal Contacts[a]

		Ag sub			Au sub			Pt sub		
		Φ/eV	χ^P	χ^A	Φ/eV	χ^P	χ^A	Φ/eV	χ^P	χ^A
Metal	Quantity	4.25	1.93	1.72	5.2	2.54	1.92	5.65	2.28	1.87
		OPD1	OPD2	OPD3	OPD1	OPD2	OPD3	OPD1	OPD2	OPD3
	$\Delta\Phi_{UPS/eV}$	0.59	0.68	0.64	−0.48	−0.48	−0.40	−0.84	−0.81	−0.88
	$\Delta\Phi_{SKPM/eV}$	0.36	0.30	0.30	−0.48	−0.43	−0.48	−1.20	−1.06	−0.99
Ag tip	Γ/meV	44.0	19.2	6.78	65.3	21.1	8.22	86.7	33.0	13.0
	$\delta(\Gamma)$/meV	1.42	0.47	1.34	1.37	0.78	0.27	2.09	0.98	0.48
Au tip	Γ/meV	68.4	21.5	8.42	142	56.6	18.3	193.6	69.6	24.7
	$\delta(\Gamma)$/meV	2.0	0.62	0.23	3.46	1.76	0.65	4.47	1.94	0.83
Pt tip	Γ/meV	87.1	33.8	12.6	189.7	64.7	25.1	317.3	109.7	40.1
	$\delta(\Gamma)$/meV	1.86	0.37	0.12	3.3	0.76	0.28	6.94	3.12	1.02
		C8DT	C9DT	C10DT	C8DT	C9DT	C10DT	C8DT	C9DT	C10DT
	$\Delta\Phi_{UPS/eV}$	−0.06	−0.15	−0.19	−0.79	−0.85	−0.87	−1.34	−1.33	−1.38
	$\Delta\Phi_{SKPM/eV}$	−0.47	−0.52	−0.43	−1.32	−1.32	−1.39	−1.77	−1.78	−1.81
Ag tip	Γ/meV	5.43	3.82	1.89	8.89	4.92	2.96	10.53	6.23	3.67
	$\delta(\Gamma)$/meV	0.39	0.21	0.05	0.49	0.35	0.16	0.66	0.53	0.26
Au tip	Γ/meV	8.68	5.05	2.90	12.93	7.38	4.85	17.40	9.98	5.59
	$\delta(\Gamma)$/meV	0.75	0.46	0.15	0.49	0.22	0.12	0.42	0.13	0.23
Pt tip	Γ/meV	10.20	6.07	3.78	17.90	9.76	5.45	25.14	14.58	7.87
	$\delta(\Gamma)$/meV	1.89	0.55	0.35	1.15	1.09	0.50	0.79	0.39	0.19

[a]The values of bare metal work functions Φ are presented along with the Pauling and Allen electronegativities $\chi^{P,A}$ in the second row. The SAM-driven changes in the work function $\Delta\Phi_{SKPM,UPS}$ measured by SKPM and UPS were reported in our previous work.[32,33,49] Each tip/substrate entry in the body of the table—namely, the average values Γ and corresponding standard errors $\delta(\Gamma)$—were deduced by averaging over ∼30 *I*−*V* measurements.

For the discussion that follows it is important to realize that the basic model parameters (ε_h, Γ_s, Γ_t, and γ) quantify microscopic properties of a molecule *embedded* in a junction, *i.e.*, a molecule having one end adsorbed on the substrate and another end adsorbed on the tip. Therefore, each of these four parameters can depend a priori on any of the three constituents of junctions (substrate, molecule (= molecular backbone + anchoring groups), tip). For example, a tip-dependent Γ_s does not violate/invalidate the single level model; Γ_s quantifies the electronic coupling between the substrate and the MO of a molecule contacted to two electrodes; and the MO properties can also depend on the tip contact. The pragmatic question addressed here is whether this theoretical possibility is quantitatively relevant in experiments.

Similar to the case of CP-AFM OPD*n* and C*n*DT junctions having electrodes of the same metal,[32,33,48] we found that eq 1 succeeds extremely well in reproducing the individual *I*−*V* traces measured for junctions with dissimilar electrodes, Figure 2. The high quality of these simulations is a strong argument for the use of the off-resonant single level model for analysis of OPD*n* and C*n*DT molecular junctions with dissimilar electrodes.

While the accurate reproduction of the experimental curves is undoubtedly important, we still want to emphasize that this is not the only reason for our reliance on this model. To make this point clearer, we note the following.

(i) The single level assumption is reasonable because we know from state-of-the-art ab initio quantum chemical calculations[49−51] (*e.g.*, based on coupled-cluster (CC) expansions[52,53] and outer valence Green's functions (OVGF)[54,55]), which go beyond the routinely employed DFT approaches, that the dominant level (HOMO) for the present molecules is well separated energetically from other MOs. Further, the values of the HOMO-Fermi offsets extracted from the measured *I*−*V* curves agree with those deduced from ultraviolet photoelectron spectroscopy (UPS).[32,33] For OPD*n*, their dependence on molecular size (*n*) exhibits the same trend as the HOMO energies obtained via quantum chemical CC calculations.[49] For C*n*DT, the HOMO energies deduced via the orSLM, which agree with those deduced via UPS, are independent of size, similar to those computed via OVGF.[33]

(ii) We did not arbitrarily pick eq 1 from a half-dozen or so available analytical formulas (*e.g.* ref 56) that express the tunneling current $I = I(V)$ mediated by a single level. The different models are deduced by assuming various energy dependencies of the transmission function (Lorentzian, Gaussian or modified Gaussian, power laws, exponential or modified exponential, etc.). The Lorentzian transmission function assumed in deriving eq 1[48] has both theoretical and experimental justification. Theoretically, the Lorentzian transmission is the direct consequence of the energy independent MO−electrode couplings $\Gamma_{s,t}$ assumed in the derivation of eq 1, which follows from the fact that typical electrode metals (Ag, Au, and Pt) possess a conduction band that is flat around the Fermi energy.[57] Experimentally, the Lorentzian shape of transmission has been demonstrated in transport, UPS, and thermopower measurements.[58]

(iii) Exploring experiment biases ($e|V| < 1.3|\varepsilon_0|$) not too close to resonance ($e|V| \approx 2|\varepsilon_0|$), we rely on eq 1 because it represents an accurate approximation of the more general expression of the tunneling current mediated by a single Lorentzian level (eqs S1a and S1f) in the SI). The reason why we prefer to use eq 1 rather than eq S1a (or eq S1f equivalent to it) is explained in detail in the SI. Briefly, letting alone the more demanding numerical effort, the latter equations do not allow extraction of more information from measured *I*−*V* data than the simpler eq 1. Importantly, neither eq S1a nor eq S1f

https://doi.org/10.1021/jacsau.4c01128
JACS Au 2025, 5, 1258−1267

can provide values for the individual MO−electrode couplings Γ_s and Γ_t.

Using appealingly simple formulas, *e.g.*, eqs 2, 4, and 6 of ref 32 ("transition voltage spectroscopy") or eq 9 of ref 59 ("five-thirds protocol"), deduced from eq 1 we can *directly* extract the values of the model parameters (ϵ_h, G, and γ) for each individual $I-V$ trace. We emphasize that, although this method can be called data fitting in a broader sense, it is not a data fitting approach in its conventional sense. We need neither guess initial values for the model parameters nor perform iterative numerical minimization converging to "best" fitting parameters that may or may not depend on how the initial values were chosen.

To directly determine the model parameters, we replot the measured $I-V$ trace as a plot of $|V^2/I|$ versus V (*e.g.*, Figure 1 in ref 42 or Figure S5 in ref 60) or $|V^{5/3}/I|$ versus V (*e.g.*, Figures 2 to 6 in ref 59) to directly extract ϵ_h. Combined with G from the low bias conductance, eq 3 provides the effective MO−electrode coupling Γ, which is the central quantity in the analysis that follows.

Data Analysis

For reasons that will become apparent below, we will focus now on the values of the effective MO−electrode coupling Γ. To compute Γ, we used $N = 80$ in eq 3, a value of the number of molecules per junction estimated in our previous studies on OPD*n*[32] and C*n*DT[33] CP-AFM junctions. In that prior work, to calculate N, we employed the state-of-the-art contact mechanics (Maugis-Dugdale model[61,62]) using values of SAM coverage measured via Rutherford backscattering and nuclear reaction analysis[63,64] as well as tip-SAM works of adhesion computed from measured rupture (pull-off) forces.[64]

The compilation of Γ values for 54 different junctions is shown in Table 1. Selected histograms for Γ are depicted in Figures S3 and S4 of the SI.

With the Γ data in hand, we turn now to our central question that, to the best of our knowledge, has not been addressed previously: does the MO electronic coupling to an electrode impact the MO electronic coupling to the other electrode? Or, more loosely, does the second electrode of a molecular junction impact the MO coupling to the first electrode?

It appears that to answer this question, information on the individual electronic MO couplings Γ_s and Γ_t is needed, and the difficulty is that separate values of Γ_s and Γ_t cannot be directly determined by fitting transport data for a given junction; what one can determine from experiment via eqs 1 and 2 is the product $\Gamma_s\Gamma_t = \Gamma^2$ (eq 3), not the individual Γ_s and Γ_t values. To reiterate, although both the product $\Gamma_s\Gamma_t$ and the sum $\Gamma_s + \Gamma_t$ enter eq S1f, this equation does not allow estimation of Γ_s and Γ_t separately (cf. Figure S2 and discussion related to it in the SI).

It turns out that even in the absence of specific values for Γ_s and Γ_t, respectively, we can still address the question above. Instead of directly comparing, *e.g.*, values of Γ_s for junctions with a given type of metal as substrate and tips of various metals, we will compare ratios of Γ^2 which would be equal if, *e.g.*, junctions with a given type of metal as substrate and tips of various metals had the same Γ_s.

To facilitate the analysis, it is convenient to rewrite eq 3 using a more precise notation for the MO−electrode couplings (Γ's). In addition to specifying CP-AFM tip or substrate (via the subscript t or s), we need notations that also indicate the nature of the two metals. So, *e.g.*, instead of simply writing Γ_s we will write Γ_s(tAg, sAu) to specify the MO coupling to the substrate of gold for a CP-AFM junction with a tip of silver. We use Γ(tAg, sAu) with no subscript for the average coupling of the same junction (cf. eq 3). For example

$$\Gamma^2(\text{tAg, sAu}) = \Gamma_s(\text{tAg, sAu})\Gamma_t(\text{tAg, sAu}) \tag{4}$$

The general notation is presented in Figure 3. A glossary of symbols is included in the SI.

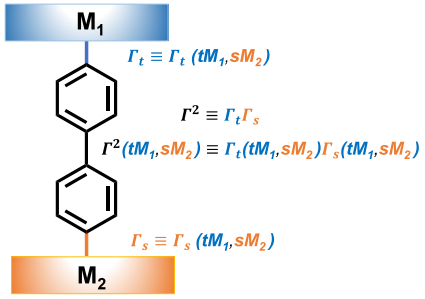

Figure 3. General notation for the MO−electrode couplings for a molecular junction having a tip (t) of metal M_1 and a substrate (s) of metal M_2.

First, we address whether the inherently asymmetric geometric shape of the CP-AFM tip and substrate makes electronic coupling to the MO asymmetric:

$$\text{Question: } \Gamma_t(\text{tM}_1, \text{sM}_2) \neq \Gamma_s(\text{tM}_2, \text{sM}_1)$$

To be specific (see eq S2 in the SI for the general case), if in a junction with one electrode of gold (M_1= Au) and the other electrode of silver (M_2= Ag) the MO−electrode electronic couplings merely depended on the nature of the metal, the following relations would be satisfied.

$$\left.\begin{aligned}\Gamma_t(\text{tAg, sAu}) &= \Gamma_s(\text{tAu, sAg})\\ \Gamma_s(\text{tAg, sAu}) &= \Gamma_t(\text{tAu, sAg})\end{aligned}\right\} \Rightarrow \Gamma^2(\text{tAg, sAu}) = \Gamma^2(\text{tAu, sAg}) \tag{5a}$$

Using the values of $\Gamma(\text{tM}_1, \text{sM}_2)$ from Table 1, we show in Figure 4 that eq 5a is satisfied by our CP-AFM OPD*n* and C*n*DT junctions. Indeed, as visible there, the left- and right-hand sides of eq 5a indeed coincide, and this is the case not only for gold (M_1 = Au) and silver (M_2= Ag) but for all pairs of metals (M_1, M_2). The MO electronic coupling to the CP-AFM tip of a given metal does not significantly differ from the MO electronic coupling to the substrate of the same metal provided the other electrode is the same. In our CP-AFM junctions with symmetric (OPD*n* and C*n*DT) molecules the electrodes are coupled symmetrically:

$$\begin{aligned}&\text{Experiment says: } \Gamma_t(\text{tM}_1, \text{sM}_2) = \Gamma_s(\text{tM}_2, \text{sM}_1)\\ &\Rightarrow \Gamma^2(\text{tM}_1, \text{sM}_2) = \Gamma^2(\text{tM}_2, \text{sM}_1)\end{aligned} \tag{5b}$$

Because eq 5b is of paramount importance for the ensuing discussion we have recast it in a more explicit form as eq S2 in the SI. A comment is in order at this point. Equations 5b and S2 mean that in our CP-AFM junctions Γ depends on metal selection only and not electrode geometry. The same message is conveyed by the panels disposed symmetrically around the diagonal in Figures S3 and S4 in the SI where selected histograms of Γ for junctions with various metal electrodes are

https://doi.org/10.1021/jacsau.4c01128
JACS Au 2025, 5, 1258−1267

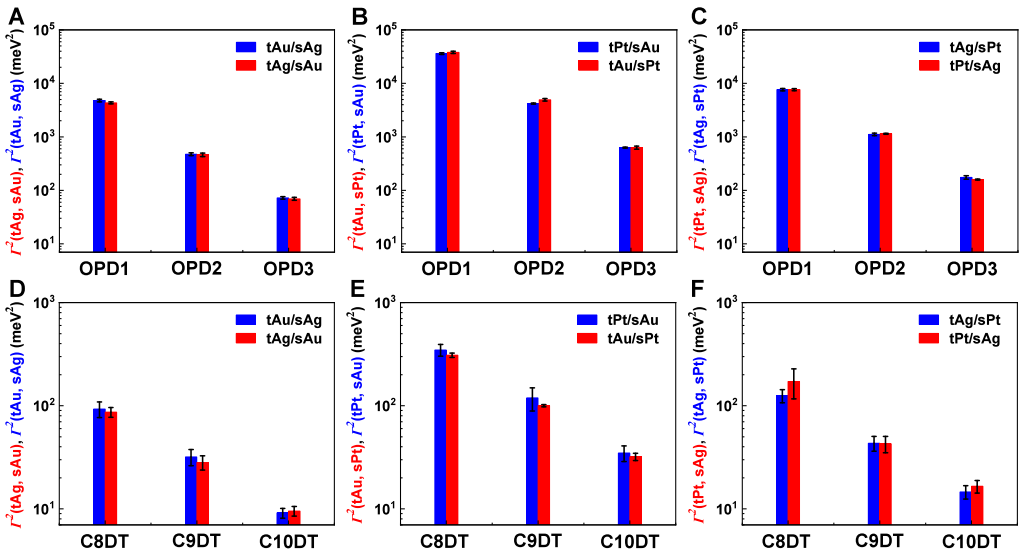

Figure 4. If a molecule's contact to the CP-AFM tip is identical to its contact to the substrate, the two values belonging to a given molecular species—(A, B, C) OPD1, OPD2, or OPD3 and (D, E, F) C8DT, C9DT or C10DT—shown in blue and red should be the same. Within standard errors (depicted by bars), the values extracted from our experimental data indeed coincide.

depicted. Intuitively, eq 5b and its more explicit counterpart eq S2 could be expected to apply for CP-AFM junctions because the tip is relatively blunt, certainly not so sharp as that of STM junctions. In our CP-AFM junctions, the tip touches the molecules with a controlled force and forms a covalent contact with an area of ∼30 nm^2.[64] When symmetric molecules are used (OPD*n* and C*n*DT with thiol on both ends), the tip covalently bonds to the molecules. The couplings $\Gamma_t(tM_1, sM_2)$ and $\Gamma_s(tM_2, sM_1)$ can be equal to each other and our data indicate that they are, within experimental error. Note the notation here carefully. We have swapped metals M_1 and M_2. We are *not* saying that $\Gamma_t(tM_1, sM_2) = \Gamma_s(tM_1, sM_2)$.

Now we move to the central question, namely whether the MO electronic coupling to one electrode is affected by the MO electronic coupling to the other electrode. We can frame it this way: does the MO electronic coupling to the tip of a given metal (*e.g.*, Ag) depend on the metal choice for the substrate electrode (X = Au, Pt in eq 6)?

$$\text{Question: } \Gamma_t(tAg, sAg) = \Gamma_t(tAg, sX)\ (X = Au, Pt) \tag{6a}$$

Rephrasing, does the MO electronic coupling to a tip of silver change if the substrate of silver is replaced by a substrate of gold or platinum?

A similar question would hold for the MO electronic coupling to the substrate of a given metal. For example

$$\text{Question: } \Gamma_s(tAg, sAg) = \Gamma_s(tX, sAg)\ (X = Au, Pt) \tag{6b}$$

Rephrasing again, does the MO electronic coupling to a substrate of silver change if the tip of silver is replaced by a tip of gold or platinum?

As noted above, Γ^2 is extracted from molecular junction experiments, and we are not able to determine the individual MO electronic couplings Γ_t and Γ_s. This means we cannot address questions like eq 6 directly. However, we show below that we can indeed compare the left- and right-hand sides of eq 6 (or the counterpart for gold and platinum substrates) indirectly by considering ratios of the "observable" Γ^2. To begin, we first define the interface feedback factor $f_{s,t}$ as follows:

$$\Gamma_t(tM, sM') = f_t(tM, sM')\Gamma_t(tM, sM) \tag{7a}$$

$$\Gamma_s(tM', sM) = f_s(tM', sM)\Gamma_s(tM, sM) \tag{7b}$$

Expressing in words what is expressed mathematically in eq 7a, $f_t(tM, sM')$ is a dimensionless factor which quantifies the change in MO coupling to the tip $\Gamma_t(tM, sM')$ in a junction tM−molecule−sM′ with dissimilar electrodes (M ≠ M′) relative to the MO coupling to the tip $\Gamma_t(tM, sM')$ in a junction tM−molecule−sM with similar electrodes. Similarly, $f_s(tM, sM')$ is a dimensionless factor accounting for the change in the MO coupling to the substrate $\Gamma_s(tM, sM')$ in a junction tM′−molecule−sM with dissimilar electrodes (M ≠ M′) relative to the MO coupling to the substrate $\Gamma_s(tM, sM')$ in a junction tM−molecule−sM with similar electrodes.

Inspection of eq 7 reveals that the departure of f_t from unity is a measure of the feedback (modification) of the MO electronic coupling to the tip when the substrate of a junction with similar electrodes (tM, sM) is replaced by another substrate (sM → sM′). Likewise, f_s quantifies the feedback of the MO electronic coupling to the substrate when the tip of a junction with similar electrodes (tM, sM) is replaced by another tip (tM → tM′). $f_{s,t} = 1$ implies the absence of interface feedback effects. We can now also see that the equalities in question in eq 6 are equivalent to asking whether $f_{s,t} = 1$ in eq 7.

With the definitions in eqs 3, 4, and 7, we can express ratios of the observables $\Gamma^2(tX, sM_1)/\Gamma^2(tX, sM_2$ as follows:

$$\frac{\Gamma^2(tX, sM_1)}{\Gamma^2(tX, sM_2)} = \frac{\Gamma_t(tX, sM_1)}{\Gamma_t(tX, sM_2)}\frac{\Gamma_s(tX, sM_1)}{\Gamma_s(tX, sM_2)}$$
$$= \frac{f_t(tX, sM_1)\Gamma_t(tX, sX)}{f_t(tX, sM_2)\Gamma_t(tX, sX)}\frac{f_s(tX, sM_1)\Gamma_s(tM_1, sM_1)}{f_s(tX, sM_2)\Gamma_s(tM_2, sM_2)}$$
$$= \frac{f_t(tX, sM_1)f_s(tX, sM_1)}{f_t(tX, sM_2)f_s(tX, sM_2)} \times \frac{\Gamma_s(tM_1, sM_1)}{\Gamma_s(tM_2, sM_2)} \tag{8a}$$

https://doi.org/10.1021/jacsau.4c01128
JACS Au 2025, 5, 1258−1267

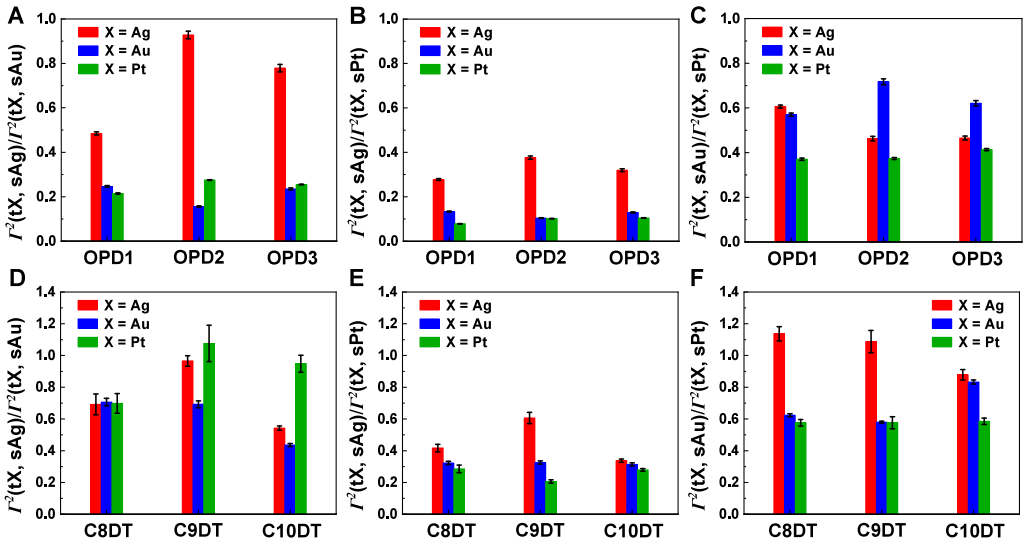

Figure 5. If the ratios of the various Γ^2 (that can be expressed in terms of the interface feedback factors $f_{s,t}$, cf. eq S4) were equal, the colored (red, blue, and green) rectangles of each of the three groups depicted with standard errors would have equal heights. In reality the heights are not equal, and this reveals a substantial mutual influence between the HOMO electronic couplings to the substrate and tip. Error bars represent standard error. (A, B, C) Results for OPD*n*. (D, E, F) Results for C*n*DT. Notice that in each of the above panels we kept the substrate electrodes fixed. Due to the invariance under metal swapping (eq 5), if we kept the tip electrodes fixed the results would coincide within statistical errors, as visible by comparing the two panels of Figure S5 among themselves.

While the individual $f_{s,t}$ values in eq 8a are not known, one can see that if $f_{s,t} = 1$, then $\Gamma^2(\mathrm{tX}, \mathrm{sM}_1)/\Gamma^2(\mathrm{tX}, \mathrm{sM}_2)$ is equal to the ratio of the Γ_s values. That is,

$$\frac{\Gamma^2(\mathrm{tX}, \mathrm{sM}_1)}{\Gamma^2(\mathrm{tX}, \mathrm{sM}_2)} \xrightarrow{f_{s,t}\equiv 1} \underbrace{\frac{\Gamma_s(\mathrm{tM}_1, \mathrm{sM}_1)}{\Gamma_s(\mathrm{tM}_2, \mathrm{sM}_2)}}_{\text{value independent of X}} \tag{8b}$$

The same argument can be made to relate $\Gamma^2(\mathrm{tX}, \mathrm{sM}_1)/\Gamma^2(\mathrm{tX}, \mathrm{sM}_2)$ (which is equal to the ratio $\Gamma^2(\mathrm{tM}_1, \mathrm{sX})/\Gamma^2(\mathrm{tM}_2, \mathrm{sX})$ by virtue of the metal swapping invariance (eq (5b)) to the ratio of Γ_t values (see eq S3b in the SI).

Importantly, inspection of eq 8b shows that the right-hand side is independent of choice of X. Since X can be Ag, Au, or Pt, one can write three equations where the right-hand side stays the same. Thus, we can write for example

$$\text{Question: } \frac{\Gamma^2(\mathrm{tAg}, \mathrm{sAg})}{\Gamma^2(\mathrm{tAg}, \mathrm{sAu})} = \frac{\Gamma^2(\mathrm{tAu}, \mathrm{sAg})}{\Gamma^2(\mathrm{tAu}, \mathrm{sAu})} = \frac{\Gamma^2(\mathrm{tPt}, \mathrm{sAg})}{\Gamma^2(\mathrm{tPt}, \mathrm{sAu})} \tag{9a}$$

A full consideration of the other metal combinations (see Supporting Information) also leads to

$$\text{Question: } \frac{\Gamma^2(\mathrm{tAg}, \mathrm{sAg})}{\Gamma^2(\mathrm{tAg}, \mathrm{sPt})} = \frac{\Gamma^2(\mathrm{tAu}, \mathrm{sAg})}{\Gamma^2(\mathrm{tAu}, \mathrm{sPt})} = \frac{\Gamma^2(\mathrm{tPt}, \mathrm{sAg})}{\Gamma^2(\mathrm{tPt}, \mathrm{sPt})} \tag{9b}$$

$$\text{Question: } \frac{\Gamma^2(\mathrm{tAg}, \mathrm{sAu})}{\Gamma^2(\mathrm{tAg}, \mathrm{sPt})} = \frac{\Gamma^2(\mathrm{tAu}, \mathrm{sAu})}{\Gamma^2(\mathrm{tAu}, \mathrm{sPt})} = \frac{\Gamma^2(\mathrm{tPt}, \mathrm{sAu})}{\Gamma^2(\mathrm{tPt}, \mathrm{sPt})} \tag{9c}$$

Evaluating whether these equalities hold is equivalent to determining whether $f_{s,t} = 1$; essentially questions 9 are equivalent to questions 6. If the equalities in questions 9 hold, then $f_{s,t} = 1$ for all metal electrode combinations, and one can say that tip-to-orbital electronic coupling does not influence substrate-to-orbital electronic coupling and vice versa.

Using the values for Γ^2 extracted from the individual $I-V$ curves measured for the various pairs of (tip, substrate) electrodes, we have depicted in Figure 5A the 3 Γ^2 ratios entering eq 9 for junctions based on OPD1, OPD2, and OPD3 with silver and gold substrates; more precisely, a total of 9 bars are shown with heights equal to the average value of the ratio and uncertainties equal to the standard error (Q and δQ, cf. eq S5 in the Supporting Information). Similar results for the OPD*n* junctions with other combinations of metal substrates (pertaining to eqs 9b and 9c) are presented in Figures 5B and 5C. Their counterparts for C*n*DT junctions are shown in Figures 5D to 5F. Inspection of Figure 5 shows that for each molecular length, OPD1−OPD3 and C8DT−C10DT, the vast majority of postulated equalities in eq 9 do not hold. For example, the quantities entering the left-hand side of eq 9a differ by those entering the right-hand side by factors of up to ∼6 (the inverse of the value ∼0.17 depicted in Figure 5A), *i.e.*, the differences are much larger than the corresponding statistical errors in the ratios of Γ^2's, which are depicted by error bars (see Supporting Information). In summary, our data do not support eq 9, and hence eq 6 also does not apply.

Experiment says, e.g.:

$$\begin{cases} \Gamma_t(\mathrm{tAg}, \mathrm{sAg}) \neq \Gamma_t(\mathrm{tAg}, \mathrm{sX})(\mathrm{X} = \mathrm{Au}, \mathrm{Pt}) \\ \Gamma_s(\mathrm{tAg}, \mathrm{sAg}) \neq \Gamma_s(\mathrm{tX}, \mathrm{sAg})(\mathrm{X} = \mathrm{Au}, \mathrm{Pt}) \end{cases}$$

This is a critical result. It says that the choice of metals for *both* electrodes is critical to the value of Γ for one interface. We call this behavior the interface feedback effect (IFB).

To explore the origins of this effect, we interrogated whether the ratios entering eq 9 correlate with the interfacial charge transfer to the contacts. Accordingly, we plotted the above ratios versus the work function of the bare metal Φ and SAM-driven change in the work function $\Delta\Phi$, as well as the metal's

https://doi.org/10.1021/jacsau.4c01128
JACS Au 2025, 5, 1258−1267

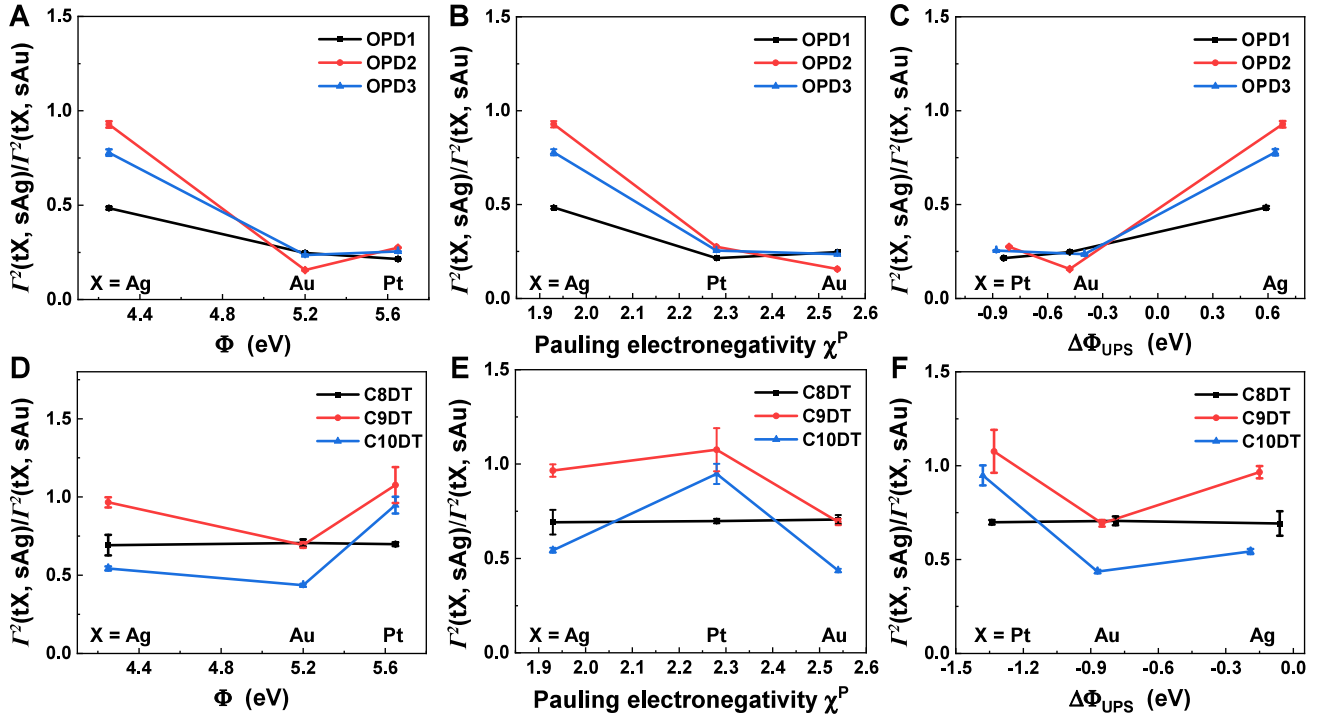

Figure 6. Ratios of Γ^2 of OPD*n* and C*n*DT depicted with standard error bars do not appear to be simply correlated with (A, D) the bare metal work function Φ, (B, E) the Pauling electronegativities χ^P, and (C, F) SAM-driven work function changes measured via UPS $\Delta\Phi_{UPS}$. Notice that the order of the metals in panels B and E is different from that in the other panels because $\chi_{Pt} < \chi_{Au}$ while, *e.g.* $\Phi_{Pt} > \Phi_{Au}$.

Pauling and Allen electronegativities $\chi^{P,A}$, Figures 6 and S6. A correlation with the aforementioned properties is not apparent. We conclude that the coupling between the HOMO and the electrodes is not localized at the interfaces. Importantly, our findings suggest that the IFB is a general effect. We observe it not only for molecular species possessing a HOMO delocalized over the entire molecule (OPD*n*) but also for those wherein the HOMO is localized at the molecular ends (C*n*DT). To be sure, whether the IFB is arguably more pronounced in the former than in the latter (an impression that the comparison of the upper and lower panels of Figure 5 might convey) is an issue that cannot be addressed at the present phenomenological level of theory. To address this, companion efforts involving microscopic quantum chemical investigations are highly desirable.

Still, surprising as it may be at first sight, the existence of an electronic communication between the two interfaces can tentatively be understood in terms of scattering theory. It expresses the fact that the (*unique*) wave function of the charge carrier (a hole in both OPD*n* and C*n*DT) traveling through the embedded molecules must simultaneously satisfy boundary conditions at either molecular end, and this makes the two metal−molecule contacts dependent on each other. This renders Γ_s a nonlocal property of a molecular *tunnel* junction depending not only on the substrate but also on the tip, and Γ_t a nonlocal property depending not only on the tip but also on the substrate.

Noteworthily, we spoke above of a "unique" wave function and of molecular "tunnel" junctions. This is not coincidental. Transport by tunneling is a unique, one-step process which implies two *coherent* charge transfer processes $L \rightarrow M$ (left electrode → molecule) and $M \rightarrow R$ (molecule → right electrode) that cannot be separate from each other. The pertaining wave function is a unique ("coherent") wave function that cannot be split into two independent components. There is no wave function of the charge carrier traveling from the substrate to the molecule distinct from a wave function of the charge carrier traveling from the molecule to the tip.

CONCLUSION

If we could extract separate values of Γ_t and Γ_s from transport measurements, we could directly compare the values of Γ_t(tAu, sAg), Γ_t(tAu, sAu), and Γ_t(tAu, sPt) for junctions with Au tips and various substrates, for example. Different values of the three aforementioned Γ_t's would be evidence for the IFB. Unfortunately, this is impossible; we can only compute $\Gamma^2 = \Gamma_t\Gamma_s$.

Our ability to observe this important IFB phenomenon comes both from analysis using the single level model that allows convenient extraction of Γ^2 values from $I-V$ data and from the use of the CP-AFM platform. The latter aspect is relevant for a 2-fold reason.

First, the CP-AFM platform allows different metals to be used as electrodes. Second, the similarity of the two contacts allowed us to conclude that Γ only depends on the metal type but not on the geometric shape. This fact, quantitatively expressed by eq 5 and S2, turned out to be an essential *technical* aid in extracting valuable physical/chemical information from ratios of Γ^2 and thereby revealing the IFB.

We expect that the interfacial coupling reported here is a general physical/chemical phenomenon. If Γ_t and Γ_s are interdependent in CP-AFM junctions, they will be interdependent in any other setup. The problem is only that we cannot demonstrate this in most setups because we cannot compute Γ_t and Γ_s separately, and we cannot conveniently vary the metal of both contacts, precluding the analysis here.

https://doi.org/10.1021/jacsau.4c01128
JACS Au 2025, 5, 1258−1267

Overall, our finding of the IFB provides another critical aspect of metal−molecule contacts that will have to be addressed by any microscopic theory of molecular tunnel junctions.

MATERIALS AND METHODS

Materials

Gold nuggets (99.999% pure) were purchased from Mowrey, Inc. (St. Paul, MN). Silver pellets (99.99% pure) were purchased from Kurt J. Lesker Co. Chromium evaporation rods and evaporation boats were purchased from R. D. Mathis (Long Beach, CA). Platinum and titanium for e-beam evaporation were purchased from Kamis, Inc. (Mahopac Falls, NY). Silicon (100) wafers were obtained from Wafer Net (San Jose, CA). Contact mode AFM tips (DNP silicon nitride probes) were purchased from Bruker AFM Probes.

Conducting Tip and Sample Preparation

Conductive AFM tips used for current measurements were prepared by coating Au or Ag at a base pressure of 10^{-7} Torr using a thermal evaporator placed in a N_2-filled glovebox. Au or Ag was deposited to a thickness of 50 nm at a rate of 0.5−1 Å/s with a ∼5 nm Cr adhesion layer. They were immediately transferred to another N_2-filled glovebox to carry out the $I-V$ measurements without exposure to air. The radius of the Au or Ag coated AFM tip is expected to be ∼50 nm. Pt coated AFM tips were prepared by sputtering. A 200 Å thick Pt film was deposited on a 50 Å Ti adhesion layer, and the coated tips were immediately transferred to the measurement glovebox. For template-stripped at Au or Ag substrates, 500 nm of Au or Ag was directly deposited onto clean Si wafers in a high vacuum e-beam evaporator. We then glued Si chips (∼1 cm^2) onto the metal surface using epoxy. The epoxy layer was cured by placing the wafers in an oven at 120 °C for 1 h. For flat Pt substrates, a 3000 Å thick layer of Pt was sputter-coated onto a clean silicon wafer at a rate of approximately 2 Å/s. On top of the Pt film, a subsequent deposition of 300 Å of Cr and 2000 Å of Au was carried out using a sputtering system. The addition of the Cr/Au film improved the adhesion between the flat Pt substrates and the cured epoxy layer, thereby enhancing the yield. The remaining steps for flat Pt substrates were the same as for flat Ag and Au substrates. The Au or Ag or Pt substrates were peeled off from the silicon surface and immersed in an ethanol solution of molecules at a concentration of ∼1 mM for 20 h. Afterward, the samples were rinsed with ethanol and dried with flowing N_2.

The detailed characterization of the OPD*n* SAMs adsorbed on metals used in this paper (SAM thickness and coverage, work function modifications, etc.) was achieved using extensive measurements via a variety of methods (XPS, ellipsometry, UPS, SKPM, Rutherford backscattering (RBS) and nuclear reaction analysis (NRA), and adhesion force measurements) as also performed in conjunction with our previous studies.[32,49,64]

Transport Measurements

Current−voltage measurements were completed by mounting the substrates in the AFM and bringing the metal-coated tip into contact with the SAM under ∼1 nN of the applied compressive load (Figure 1B). Voltages were applied to the tip with a Keithley model 236 source-measure unit operated in "DC mode". Voltage was swept at the tip; the sample was grounded; and current−voltage characteristics were recorded ($V > 0$ means positive voltage on the tip). All measured $I-V$ curves crossed over from practically linear at low biases to gradually more nonlinear at higher biases. The slope of the linear portion of the $I-V$ characteristic was used to determine a junction (low bias) conductance G. Voltage sweeps to 1.2−1.5 V were applied to observe the pronounced nonlinear ($I-V$) behavior (Figures 2 and S1).

ASSOCIATED CONTENT

Supporting Information

The Supporting Information is available free of charge at https://pubs.acs.org/doi/10.1021/jacsau.4c01128.

Glossary of symbols, additional theoretical details, and figures as mentioned in the text (PDF)

AUTHOR INFORMATION

Corresponding Authors

Ioan Bâldea − *Theoretical Chemistry, Heidelberg University, D-69120 Heidelberg, Germany;* orcid.org/0000-0003-4860-5757; Email: ioan.baldea@pci.uni-heidelberg.de

C. Daniel Frisbie − *Department of Chemical Engineering and Materials Science and Department of Chemistry, University of Minnesota, Minneapolis, Minnesota 55455, United States;* orcid.org/0000-0002-4735-2228; Email: frisbie@umn.edu

Zuoti Xie − *Department of Materials Science and Engineering, Guangdong Provincial Key Laboratory of Materials and Technologies for Energy Conversion, Guangdong Technion-Israel Institute of Technology, Shantou, Guangdong 515063, China; Quantum Science Center of Guangdong-Hong Kong-Macao Greater Bay Area (Guangdong), Shenzhen-Hong Kong International Science and Technology Park, Shenzhen, Guangdong 518000, China;* orcid.org/0000-0002-1828-0122; Email: zuoti.xie@gtiit.edu.cn

Authors

Yunxia Feng − *Department of Materials Science and Engineering, Guangdong Provincial Key Laboratory of Materials and Technologies for Energy Conversion, Guangdong Technion-Israel Institute of Technology, Shantou, Guangdong 515063, China; Schulich Faculty of Chemistry, Technion-Israel Institute of Technology, Haifa 3200003, Israel;* orcid.org/0009-0007-6229-6483

Jinwei Chen − *Department of Materials Science and Engineering, Guangdong Provincial Key Laboratory of Materials and Technologies for Energy Conversion, Guangdong Technion-Israel Institute of Technology, Shantou, Guangdong 515063, China*

Complete contact information is available at: https://pubs.acs.org/10.1021/jacsau.4c01128

Notes

The authors declare no competing financial interest.

ACKNOWLEDGMENTS

Z.X. acknowledges primary financial support from the National Key R&D Program of China (2023YFA1407100), the National Natural Science Foundation of China (22373026), and the Guangdong Science and Technology Department (2021B0301030005, 2022A1515011843, 2021QN02X538 and STKJ2023072) and Guangdong Quantum Science Strategic Special Project (GDZX2304005). I.B. acknowledges computational support by the state of Baden-Württemberg through bwHPC and the German Research Foundation through Grant No. INST 40/575-1 FUGG (bwUniCluster 2.0, bwForCluster/HELIX, and JUSTUS 2.0 cluster). C.D.F. thanks the US National Science Foundation for funding under CHE-2304763.

REFERENCES

(1) Reed, M. A.; Zhou, C.; Muller, C. J.; Burgin, T. P.; Tour, J. M. Conductance of a Molecular Junction. *Science* **1997**, *278*, 252−254.
(2) Wold, D. J.; Frisbie, C. D. Formation of Metal-Molecule-Metal Tunnel Junctions: Microcontacts to Alkanethiol Monolayers with a Conducting AFM Tip. *J. Am. Chem. Soc.* **2000**, *122*, 2970−2971.
(3) Chabinyc, M. L.; Chen, X.; Holmlin, R. E.; Jacobs, H.; Skulason, H.; Frisbie, C. D.; Mujica, V.; Ratner, M. A.; Rampi, M. A.; Whitesides, G. M. Molecular Rectification in a Metal-Insulator-Metal Junction Based on Self-Assembled Monolayers. *J. Am. Chem. Soc.* **2002**, *124*, 11730−11736.
(4) Reichert, J.; Ochs, R.; Beckmann, D.; Weber, H. B.; Mayor, M.; von Löhneysen, H. Driving Current through Single Organic Molecules. *Phys. Rev. Lett.* **2002**, *88*, 176804.
(5) Xu, B.; Xiao, X.; Tao, N. J. Measurement of Single-Molecule Resistance by Repeated Formation of Molecular Junctions. *J. Am. Chem. Soc.* **2003**, *125*, 16164−16165.
(6) Yan, C.; Fang, C.; Gan, J.; Wang, J.; Zhao, X.; Wang, X.; Li, J.; Zhang, Y.; Liu, H.; Li, X.; Bai, J.; Liu, J.; Hong, W. From Molecular Electronics to Molecular Intelligence. *ACS Nano* **2024**, *18*, 28531−28556.
(7) McCreery, R. L. Molecular Electronic Junctions. *Chem. Mater.* **2004**, *16*, 4477−4496.
(8) Venkataraman, L.; Klare, J. E.; Nuckolls, C.; Hybertsen, M. S.; Steigerwald, M. L. Dependence of Single-Molecule Junction Conductance on Molecular Conformation. *Nature* **2006**, *442*, 904−907.
(9) Lörtscher, E.; Weber, H. B.; Riel, H. Statistical Approach to Investigating Transport Through Single Molecules. *Phys. Rev. Lett.* **2007**, *98*, 176807.
(10) Martin, C. A.; Smit, R. H. M.; Van Der Zant, H. S. J.; Van Ruitenbeek, J. M. A Nanoelectromechanical Single-Atom Switch. *Nano Lett.* **2009**, *9*, 2940−2945.
(11) Dief, E. M.; Low, P. J.; Díez-Pérez, I.; Darwish, N. Advances in Single-Molecule Junctions as Tools for Chemical and Biochemical Analysis. *Nat. Chem.* **2023**, *15*, 600−614.
(12) Aragonès, A. C.; Martín-Rodríguez, A.; Aravena, D.; Puigmartí-Luis, J.; Amabilino, D. B.; Aliaga-Alcalde, N.; González-Campo, A.; Ruiz, E.; Díez-Pérez, I. Tuning Single-Molecule Conductance in Metalloporphyrin-Based Wires via Supramolecular Interactions. *Angew. Chem., Int. Ed.* **2020**, *59*, 19193−19201.
(13) Qiao, X.; Sil, A.; Sangtarash, S.; Smith, S. M.; Wu, C.; Robertson, C. M.; Nichols, R. J.; Higgins, S. J.; Sadeghi, H.; Vezzoli, A. Nuclear Magnetic Resonance Chemical Shift as a Probe for Single-Molecule Charge Transport. *Angew. Chem., Int. Ed.* **2024**, *63*, e202402413.
(14) Ward, J. S.; Vezzoli, A.; Wells, C.; Bailey, S.; Jarvis, S. P.; Lambert, C. J.; Robertson, C.; Nichols, R. J.; Higgins, S. J. A Systematic Study of Methyl Carbodithioate Esters as Effective Gold Contact Groups for Single-Molecule Electronics. *Angew. Chem., Int. Ed.* **2024**, *63*, e202403577.
(15) Gu, M. W.; Peng, H. H.; Chen, I. W. P.; Chen, C. H. Tuning Surface d Bands with Bimetallic Electrodes to Facilitate Electron Transport across Molecular Junctions. *Nat. Mater.* **2021**, *20*, 658−664.
(16) Yoon, H. J.; Liao, K. C.; Lockett, M. R.; Kwok, S. W.; Baghbanzadeh, M.; Whitesides, G. M. Yoon H J, Liao K C, Lockett M R, et al. Rectification in Tunneling Junctions: 2,2'-Bipyridyl-Terminated n-Alkanethiolates. *J. Am. Chem. Soc.* **2014**, *136*, 17155−17162.
(17) Bayat, A.; Lacroix, J. C.; McCreery, R. L. Control of Electronic Symmetry and Rectification Through Energy Level Variations in Bilayer Molecular Junctions. *J. Am. Chem. Soc.* **2016**, *138*, 12287−12296.
(18) Metzger, R. M. Quo Vadis, Unimolecular Electronics? *Nanoscale* **2018**, *10*, 10316−10332.
(19) Nijhuis, C. A.; Reus, W. F.; Whitesides, G. M. Molecular Rectification in Metal-SAM-Metal Oxide-Metal Junctions. *J. Am. Chem. Soc.* **2009**, *131*, 17814−17827.
(20) Pobelov, I. V.; Li, Z.; Wandlowski, T. Electrolyte Gating in Redox-Active Tunneling Junctions—An Electrochemical STM Approach. *J. Am. Chem. Soc.* **2008**, *130*, 16045−16054.
(21) Song, H.; Kim, Y.; Jang, Y. H.; Jeong, H.; Reed, M. A.; Lee, T. Observation of Molecular Orbital Gating. *Nature* **2009**, *462*, 1039−1043.
(22) Meng, L.; Xin, N.; Hu, C.; Al Sabea, H.; Zhang, M.; Jiang, H.; Ji, Y.; Jia, C.; Yan, Z.; Zhang, Q.; Gu, L.; He, X.; Selvanathan, P.; Norel, L.; Rigaut, S.; Guo, H.; Meng, S.; Guo, X. Dual-gated Single-molecule Field-effect Transistors Beyond Moore's Law. *Nat. Commun.* **2022**, *13*, 1410.
(23) Bai, J.; Daaoub, A.; Sangtarash, S.; Li, X.; Tang, Y.; Zou, Q.; Sadeghi, H.; Liu, S.; Huang, X.; Tan, Z.; Liu, J.; Yang, Y.; Shi, J.; Mészáros, G.; Chen, W.; Lambert, C.; Hong, W. Anti-Resonance Features of Destructive Quantum Interference in Single-Molecule Thiophene Junctions Achieved by Electrochemical Gating. *Nat. Mater.* **2019**, *18*, 364−369.
(24) Li, Y.; Buerkle, M.; Li, G.; Rostamian, A.; Wang, H.; Wang, Z.; Bowler, D. R.; Miyazaki, T.; Xiang, L.; Asai, Y.; Zhou, G.; Tao, N. Gate Controlling of Quantum Interference and Direct Observation of Anti-Resonances in Single Molecule Charge Transport. *Nat. Mater.* **2019**, *18*, 357−363.
(25) Jia, C.; Migliore, A.; Xin, N.; Huang, S.; Wang, J.; Yang, Q.; Wang, S.; Chen, H.; Wang, D.; Feng, B.; Liu, Z.; Zhang, G.; Qu, D.-H.; Tian, H.; Ratner, M. A.; Xu, H. Q.; Nitzan, A.; Guo, X. Covalently Bonded Single-Molecule Junctions with Stable and Reversible Photoswitching. *Science* **2016**, *352*, 1443−1445.
(26) McCreery, R. L.; Yan, H.; Bergren, A. J. A Critical Perspective on Molecular Electronic Junctions: There is Plenty of Room in the Middle. *Phys. Chem. Chem. Phys.* **2013**, *15*, 1065−1081.
(27) Xiang, D.; Wang, X.; Jia, C.; Lee, T.; Guo, X. Molecular-Scale Electronics: From Concept to Function. *Chem. Rev.* **2016**, *116*, 4318−4440.
(28) Li, R.; Lu, Z.; Cai, Y.; Jiang, F.; Tang, C.; Chen, Z.; Zheng, J.; Pi, J.; Zhang, R.; Liu, J.; Chen, Z. B.; Yang, Y.; Shi, J.; Hong, W.; Xia, H. Switching of Charge Transport Pathways via Delocalization Changes in Single-Molecule Metallacycles Junctions. *J. Am. Chem. Soc.* **2017**, *139*, 14344−14347.
(29) Yang, Z.; Cazade, P. A.; Lin, J. L.; Cao, Z.; Chen, N.; Zhang, D.; Duan, L.; Nijhuis, C. A.; Thompson, D.; Li, Y. High Performance Mechano-Optoelectronic Molecular Switch. *Nat. Commun.* **2023**, *14*, 5639.
(30) Hnid, I.; Yassin, A.; Arbouch, I.; Guérin, D.; Van Dyck, C.; Sanguinet, L.; Lenfant, S.; Cornil, J.; Blanchard, P.; Vuillaume, D. Molecular Junctions for Terahertz Switches and Detectors. *Nano Lett.* **2024**, *24*, 2553−2560.
(31) Smith, C. E.; Xie, Z.; Bâldea, I.; Frisbie, C. D. Work Function and Temperature Dependence of Electron Tunneling Through an N-Type Perylene Diimide Molecular Junction with Isocyanide Surface Linkers. *Nanoscale* **2018**, *10*, 964−975.
(32) Xie, Z.; Bâldea, I.; Frisbie, C. D. Determination of Energy-Level Alignment in Molecular Tunnel Junctions by Transport and Spectroscopy: Self-Consistency for the Case of Oligophenylene Thiols and Dithiols on Ag, Au, and Pt Electrodes. *J. Am. Chem. Soc.* **2019**, *141*, 3670−3681.
(33) Xie, Z.; Bâldea, I.; Frisbie, C. D. Energy Level Alignment in Molecular Tunnel Junctions by Transport and Spectroscopy: Self-Consistency for the Case of Alkyl Thiols and Dithiols on Ag, Au, and Pt Electrodes. *J. Am. Chem. Soc.* **2019**, *141*, 18182−18192.
(34) Salomon, A.; Cahen, D.; Lindsay, S.; Tomfohr, J.; Engelkes, V. B.; Frisbie, C. D. Comparison of Electronic Transport Measurements on Organic Molecules. *Adv. Mater.* **2003**, *15*, 1881−1890.
(35) Kim, T.; Vázquez, H.; Hybertsen, M. S.; Venkataraman, L. Conductance of Molecular Junctions Formed with Silver Electrodes. *Nano Lett.* **2013**, *13*, 3358−3364.
(36) Akkerman, H. B.; de Boer, B. Electrical Conduction through Single Molecules and Self-Assembled Monolayers. *J. Phys.: Condens. Matter* **2008**, *20*, 013001.

https://doi.org/10.1021/jacsau.4c01128
JACS Au 2025, 5, 1258−1267

(37) Sangeeth, C. S. S.; Demissie, A. T.; Yuan, L.; Wang, T.; Frisbie, C. D.; Nijhuis, C. A. Comparison of DC and AC Transport In 1.5−7.5 nm Oligophenylene Imine Molecular Wires across Two Junction Platforms: Eutectic Ga-In versus Conducting Probe Atomic Force Microscope Junctions. *J. Am. Chem. Soc.* **2016**, *138*, 7305−7314.
(38) Heimel, G.; Romaner, L.; Zojer, E.; Bredas, J. L. Toward Control of the Metal-Organic Interfacial Electronic Structure in Molecular Electronics: A First-Principles Study on Self-Assembled Monolayers of π-Conjugated Molecules on Noble Metals. *Nano Lett.* **2007**, *7*, 932−940.
(39) Diez-Cabanes, V.; Gonzalez, S. R.; Osella, S.; Cornil, D.; Van Dyck, C.; Cornil, J. Energy Level Alignment at Interfaces between Au (111) and Thiolated Oligophenylenes of Increasing Chain Size: Theoretical Evidence of Pinning Effects. *Adv. Theory Simul.* **2018**, *1*, 1700020.
(40) Zhang, G.; Ratner, M. A.; Reuter, M. G. Is Molecular Rectification Caused by Asymmetric Electrode Couplings or by a Molecular Bias Drop. *J. Phys. Chem. C* **2015**, *119*, 6254−6260.
(41) Bâldea, I. Why Asymmetric Molecular Coupling to Electrodes Cannot Be at Work in Real Molecular Rectifiers. *Phys. Rev. B* **2021**, *103*, 195408.
(42) Bâldea, I.; Xie, Z.; Frisbie, C. D. Uncovering a Law of Corresponding States for Electron Tunneling in Molecular Junctions. *Nanoscale* **2015**, *7*, 10465−10471.
(43) Schmickler, W. Investigation of Electrochemical Electron Transfer Reactions with a Scanning Tunneling Microscope: A Theoretical Study. *Surf. Sci.* **1993**, *295*, 43−56.
(44) Stafford, C. A. Nonlinear Conductance in Resonant Tunneling. *Phys. Rev. Lett.* **1996**, *77*, 2770−2773.
(45) Haug, H.; Jauho, A.-P. *Quantum Kinetics in Transport and Optics of Semiconductors*, 2nd ed.; Springer-Verlag: Berlin Heidelberg, 2008.
(46) Hall, L. E.; Reimers, J. R.; Hush, N. S.; Silverbrook, K. Formalism, Analytical Model, and a Priori Green's-Function-Based Calculations of the Current-Voltage Characteristics of Molecular Wires. *J. Chem. Phys.* **2000**, *112*, 1510−1521.
(47) Peterson, I. R.; Vuillaume, D.; Metzger, R. M. Analytical Model for Molecular-Scale Charge Transport. *J. Phys. Chem. A* **2001**, *105*, 4702−4707.
(48) Bâldea, I. Ambipolar Transition Voltage Spectroscopy: Analytical Results and Experimental Agreement. *Phys. Rev. B* **2012**, *85*, 035442.
(49) Xie, Z.; Bâldea, I.; Smith, C. E.; Wu, Y.; Frisbie, C. D. Experimental and Theoretical Analysis of Nanotransport in Oligophenylene Dithiol Junctions as a Function of Molecular Length and Contact Work Function. *ACS Nano* **2015**, *9*, 8022−8036.
(50) Xie, Z.; Bâldea, I.; Frisbie, C. D. Why One Can Expect Large Rectification in Molecular Junctions Based on Alkane Monothiols and Why Rectification Is So Modest. *Chem. Sci.* **2018**, *9*, 4456−4467.
(51) Xie, Z.; Bâldea, I.; Van Nguyen, Q.; Frisbie, C. D. Quantitative Analysis of Weak Current Rectification in Molecular Tunnel Junctions Subject to Mechanical Deformation Reveals Two Different Rectification Mechanisms for Oligophenylene Thiols versus Alkane Thiols. *Nanoscale* **2021**, *13*, 16755−16768.
(52) Stanton, J. F.; Bartlett, R. J. The Equation of Motion Coupled-Cluster Method: A Systematic Biorthogonal Approach to Molecular Excitation Energies, Transition Probabilities, and Excited State Properties. *J. Chem. Phys.* **1993**, *98*, 7029−7039.
(53) Stanton, J. F.; Gauss, J. Analytic Energy Derivatives for Ionized States Described by the Equation-of-Motion Coupled Cluster Method. *J. Chem. Phys.* **1994**, *101*, 8938−8944.
(54) Cederbaum, L. S. One-Body Green's Function for Atoms and Molecules: Theory and Application. *J. Phys. B At. Mol. Phys.* **1975**, *8*, 290−303.
(55) von Niessen, W.; Schirmer, J.; Cederbaum, L. S. Computational Methods for the One-Particle Green's Function. *Comput. Phys. Rep.* **1984**, *1*, 57−125.
(56) Bâldea, I. Important Issues Facing Model-Based Approaches to Tunneling Transport in Molecular Junctions. *Phys. Chem. Chem. Phys.* **2015**, *17*, 20217−20230.
(57) Papaconstantopoulos, D. A. *Handbook of the Band Structure of Elemental Solids*; Springer US: Boston, MA, 2015.
(58) Bâldea, I. Evidence That Molecules in Molecular Junctions May Not Be Subject to the Entire External Perturbation Applied to Electrodes. *Langmuir* **2020**, *36*, 1329−1337.
(59) Bâldea, I. Gaining Insight into Molecular Tunnel Junctions with a Pocket Calculator Without I-V Data Fitting: Five-Thirds Protocol. *Phys. Chem. Chem. Phys.* **2024**, *26*, 8724−8733.
(60) Xie, Z.; Bâldea, I.; Oram, S.; Smith, C. E.; Frisbie, C. D. Effect of Heteroatom Substitution on Transport in Alkanedithiol-Based Molecular Tunnel Junctions: Evidence for Universal Behavior. *ACS Nano* **2017**, *11*, 569−578.
(61) Maugis, D. Adhesion of Spheres: The JKR-DMT Transition Using a Dugdale Model. *J. Colloid Interface Sci.* **1992**, *150*, 243−269.
(62) Dugdale, D. S. Yielding of Steel Sheets Containing Slits. *J. Mech. Phys. Solids* **1960**, *8*, 100−104.
(63) Demissie, A. T.; Haugstad, G.; Frisbie, C. D. Quantitative Surface Coverage Measurements of Self-Assembled Monolayers by Nuclear Reaction Analysis of Carbon-12. *J. Phys. Chem. Lett.* **2016**, *7*, 3477−3481.
(64) Xie, Z.; Bâldea, I.; Demissie, A. T.; Smith, C. E.; Wu, Y.; Haugstad, G.; Frisbie, C. D. Exceptionally Small Statistical Variations in the Transport Properties of Metal-Molecule-Metal Junctions Composed of 80 Oligophenylene Dithiol Molecules. *J. Am. Chem. Soc.* **2017**, *139*, 5696−5699.

https://doi.org/10.1021/jacsau.4c01128
JACS Au 2025, 5, 1258−1267